

No evidence for Keplerian taper of far-out galactic rotation

Adriana Bariego Quintana^a and Felipe J. Llanes-Estrada^b

^a*Instituto de Fisica Corpuscular, Paterna, E-46980, Valencia, Spain*

^b*Dept. Fisica Teorica & IPARCOS, Univ. Complutense de Madrid, Madrid, E-28040, , Spain*

Abstract

We present a statistical analysis of the 175 SPARC galactic rotation curves to test the hypothesis of whether the Keplerian velocity tapering at large radii ($v(r) \propto 1/\sqrt{r}$) of the Navarro-Frenk-White (NFW) halo model agrees with observational data. The null hypothesis is Rubin's flat-rotation curve, $v(r) = \text{constant}$ -such as can be obtained from a spherical, isothermal-like density profile, or alternatively with a very prolate halo-. To decide whether we adopt the null (Rubin behaviour) or alternative (NFW behaviour) hypothesis, we evaluate the derivative in each galaxy of $v(r)$ with its last data points. We conclude that the data is presently compatible with the null hypothesis -no taper off, no decline of $v(r)$ is seen.

1. Introduction

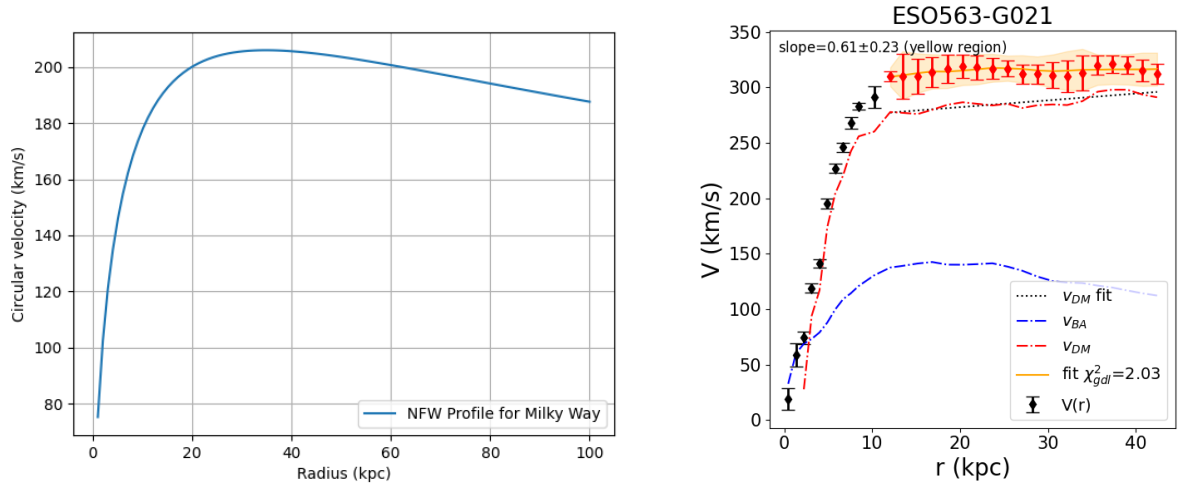


Figure 1: **Left:** Dark-Matter induced rotation curve within the Milky Way's supposed in a spherical NFW halo. At distances from the center doubling that of the local maximum, the velocity curve clearly displays the Keplerian $1/\sqrt{r}$ fall-off. **Right:** Example galaxy with well measured rotation curve that does not fall-off but rather flattens out (shaded area) at large radius (even past three to four times the would-be maximum) in contrast to the NFW prediction. This apparent shape disagreement motivates our study.

There is a trove of observational evidence for an unidentified gravitating component in the Universe (Profumo, 2017), from galactic to cluster to Hubble scales, so that even the power spectrum of the Cosmic Background radiation informs us about the need for such an extra component (Efstathiou et al., 2020), also necessary to explain today's large scale structure formation.

While extensions of gravitational theories (Milgrom, 1983) are still discussed, a leading hypothesis posits that large-scale observations are best explained by a new component of matter, Dark Matter (DM) (Bertone and Hooper, 2018).

According to Cosmic Structure formation, Dark Matter created large potential wells during the first stages of the Universe, to then pull baryonic matter and start structure formation (Dodelson and Liguori, 2006). Cosmological simulations suggest that in the present universe galaxies are surrounded by Dark Matter haloes that alter probe-mass trajectories.

Without speculating about the nature of this gravitating component, one can aim to constrain the potential of DM haloes to understand their shape, distribution, and underlying properties (Bariego-Quintana and Llanes-Estrada, 2024a), for example from stellar streams (Walder et al., 2024). Of the abundant observational evidence supporting the existence of Dark matter, the indefinitely flat rotation curve seen in a large fraction of galaxies –as studied in depth by V. Rubin and Collaborators in the 1970s (Rubin et al., 1978)– stands out for its simplicity.

Standard theoretical analysis assumes a spherical Dark Matter halo. Fitting the matter concentrations in cosmological simulations (Di Cintio et al., 2014) leads to functions such as the isothermal Navarro-Frenk-White (NFW) (Navarro et al., 1997) which, for a galaxy like the Milky Way, can be written as the following density profile

$$\rho_{NFW} = \frac{\rho_0}{x \cdot (1 + x)^2} \quad (1)$$

where $x = r/r_0$ for $r_0 = 16.1 \text{ kpc}$ is the distance at which $\text{dlog } \rho / \text{dlog } r = -2$ and $\rho_0 = 1.4 \cdot 10^{-7} M_\odot / \text{kpc}^3$ is the local dark matter density at Earth. The rotation curve $v(r)$ for such a spherical NFW halo is easily derived from orbital equilibrium,

$$V(r) = \sqrt{\frac{4\pi G}{r} \int_0^r dr' r'^2 \rho_{NFW}(r')} = \sqrt{\frac{4\pi G}{x} \rho_0 r_0^2 \left[\ln |1 + x| - \frac{x}{1 + x} \right]}. \quad (2)$$

In Figure 1 opening the article we observe the behaviour of the DM rotation curve for the Milky Way NFW spherical halo using Eq. 2 with parameters obtained from (Nesti and Salucci, 2013). The maximum velocity is found at a radius $r = 34.3 \text{ kpc}$, and for larger radii this model $v(r)$ function shows a slight declining behavior: at 40 kpc the DM rotation curve will have decreased a 1% with respect to the maximum, at 50 kpc a 10% and at 60 an 18%, starting to show the $v(r) \propto 1/\sqrt{r}$ characteristic of Keplerian orbits because most of the halo mass is already inside the orbit.

On the contrary, many galaxies show the behaviour found by Rubin and collaborators, as exemplified on the right panel of the same Figure 1: no such tapering is visible in the velocity function.

Because the baryonic-mass distribution in the Milky Way is known to distances of $\sim 50 \text{ kpc}$, and is well confined, in the external regions of the galaxy the centripetal force contributed by baryons is typically subdominant and returns the expected velocity decreasing as $r^{-1/2}$; therefore, we do not expect the baryonic component of Milky-way like galaxies contributing significantly to the observed flattening. The sufficiency of the spherical NFW profile in explaining such rotation-curve flattening remains questionable ¹.

Pushing to still larger distances, a recent study extended the would-be rotation curve of four galaxies to distances of hundreds of kpc and even a Mpc using weak gravitational lensing (Mistele et al., 2024). That work concluded that the rotation curves at those extreme distances, if they could be directly measured, would continue to show constant $v(r)$ rotation velocity, unlike a spherical halo with an isothermal Navarro-Frenk-White density profile (Frenk et al., 1985).

Our intention in this work is to evaluate whether the further-most part of the rotation curve does start decreasing or not, running a sufficient statistical analysis of the well-measured SPARC-database galaxies (Lelli et al., 2016). There, galactic rotation curves measured from the Doppler Effect in the H1 and H α lines for 175 spiral and irregular galaxies are provided. Additionally, the baryonic component rotation curves for the gas, bulge and disk of each are estimated based on surface photometry of galaxies at $3.6 \mu\text{m}$. The baryonic rotation curve is the result of the squared sum of all:

$$v_{BA} = \sqrt{v_{bulge}^2 + v_{gas}^2 + v_{disk}^2}. \quad (3)$$

¹The only spherically-symmetric viable mass distribution in those outer galactic confines is the power-law $\rho \propto r^{-2}$, fine-tuned to precisely that exponent, only explainable if one accepts a thermalized halo, another questionable assumption given that the microscopic DM properties are unknown. Alternatively, one can opt to accept prolate or even cylindrical sources of gravity, which would make the constant $v(r)$ natural outside the DM distribution (Llanes-Estrada, 2021; Bariego-Quintana et al., 2023; Bariego-Quintana and Llanes-Estrada, 2024b).

When accounting for a presumed DM halo, there is an additional contribution to the total rotation curve, v_{DM} , which is also added in quadrature (because the corresponding centripetal force is added linearly and $F_c \propto v^2$),

$$v = \sqrt{v_{DM}^2 + v_{BA}^2}. \quad (4)$$

In Section 2 the set of galaxies is trimmed off irrelevant ones for the analysis (mostly because of their measurements being too close to the galactic center), and statistical tests are deployed to decide on whether the slope $v'(r)|_{r=r_{\max}}$ is negative (as predicted by the NFW model) or compatible with zero.

First, in Subsec. 2.1 we evaluate the slope at the end of the galactic disk, a distance at which only small quantities of baryonic matter are expected. This proceeds by fitting a linear function to the last points of the Dark Matter rotation curve. Then, in Subsec. 2.2, we study $v'(r)$ to understand whether a general downsloping trend for the rotation velocity in galaxies is obeyed by the last points or whether $v(r)$ remains flat until very distant radii. In Subsec. 2.3 we select appropriate hypothesis tests to study the general trend preferred by the galactic rotation curves in the selected sample. The results of the analysis are then given in Section 3, and we summarize in Section 4.

2. Methodology

In this section we fit the last data points of the Dark Matter rotation curve $v(r)$ for each galaxy to ascertain whether their general trend is a decrease or rather a constant value of v . The largest- r points will be fit to a linear function

$$v(r) = A \cdot r + B, \quad (5)$$

using χ^2 minimization. Then we perform a hypothesis test where our null hypothesis is the null slope $v' = A = 0$ and the alternative hypothesis a negative slope $A < 0$.

2.1. Selection of galaxies

The first (and simplest to understand) requirement to be met is that the total rotation curve, in the largest- r data points, is not dominated by the baryonic matter of the galaxy. That is, the baryonic rotation curve from Eq. (3) must then be less significant than the v_{DM} that we infer from Eq. (4). This condition avoids difficult behaviours resulting from the internal galactic structure, where the shape-richer baryonic contribution to the rotation curve can be larger than the dark matter one, and keeping such galaxies or such points within a galaxy would introduce spurious pieces to the DM halo distribution which is to be studied, and which should be dominant at the edge of the galactic disk and beyond if the NFW model applies.

The second condition is less straightforward. We wish to avoid human selection bias in deciding which points are to be included in each rotation curve, since the galaxies in the database are of different sizes and sampled at different r intervals. We thus need an automated selection criterion for the last data points in each (total) rotation curve which can be applied to all galaxies without human intervention.

For each galaxy in the SPARC data set with $v(r)$ sampled at n data points, we select all possible subsets of four consecutive data points: $[S_1, S_2, \dots] = [[v_{i+1}, \dots, v_{i+4}], \dots]$ for $i = 0, n-4$. Then, we fit each subset S_j to the linear function of Eq. (5) with two free parameters $\{A, B\}$ using a χ^2 function that we minimise:

$$\chi^2 = \frac{(v_{\text{theoretical}} - v_{\text{data}})^2}{\sigma_{\text{data}}^2(v)} \quad (6)$$

where $v_{\text{theoretical}}$ is the linear parametrization (fittable function) and the velocity v_{data} , and uncertainty $\sigma(v)$ are taken from the database. The χ^2 minimization is performed by the least square method on each subset S_1, S_2, \dots , proceeding from left (lowest r) to right (highest r) until the slope A satisfies the condition

$$A \leq A_{\max} = 0.9 \text{ km/(s kpc)}. \quad (7)$$

Given that typical galaxies have velocities of order of magnitude 100 km/s and size tens of kiloparsecs, when we reach this slope level (ten times smaller than the typical average ones over the entire range) we reasonably know that we are near the maximum of the $v(r)$ curve if there is one. The criterion is uniformly applied to the entire database to reduce data selection bias. The numerical sensitivity to the particular choice of A_{\max} in Eq. (7) will be given below in Subsection 3.1.

Once the slope of $v(r)$ has decreased to the level of Eq. (7), we discard the data points that belong to subsets with smaller i indices (thus having smaller r), namely $\bigcup S_{j \leq i} = [v_0, \dots, v_i]$ and keep the rest, $\bigcup S_f = S_{\text{total}} - \bigcup S_j = [v_{i+1}, \dots, v_n]$. As an example, in Figure 1 the kept data points are shown in red. This procedure should ensure a reasonably consistent selection of the “final” few points of each rotation curve across the galaxy database. After the velocity slope decreases to this low value, we should reasonably be able to discern whether it keeps sliding below zero and becomes negative (Keplerian taper) or whether it remains consistent with zero, and learn about the asymptotic trend of velocity curves.

It is important to note that in imposing these two conditions, (1) DM dominated rotation and (2) decreased slope, we will have discarded a good number of galaxies, by the second condition those in which the rotation curve is monotonously increasing and never becomes constant or decreasing, indicating that the data was taken still deeply inside the matter/DM distribution.

2.2. Fitting method

At this point we are left with a new set of data points $S_f = [v_{i+1}, v_n]$ for each of the remaining galaxies. The next step will be to make a fit of these fragments of rotation curves, but this time we consider the Dark Matter component instead of the total rotation curve. We use Eq. (4), the baryonic component v_{BA} is taken from Eq. (3) and the DM contribution will be fitted to a linear function of this type

$$v = A \cdot r + B. \quad (8)$$

performing the least square minimisation method of the χ^2 function

$$\chi^2 = \frac{(v_{\text{theoretical}} - v_{\text{data}})^2}{\sigma_{\text{data}}^2(v)}. \quad (9)$$

We aim at optimising the slope of each $v(r)$ and at understanding its behaviour in every galaxy of this data set.

2.3. Hypothesis testing

To probe the distribution of the fitted $v'(r)$ slopes over the galaxy sample, $[A_1, A_2, \dots, A_N]$, we will employ two statistical tests with two hypotheses each, as follows:

	Parametric: Z test assuming a normal distribution	Non-parametric, agnostic about distribution
$H_0 :$	$A \geq 0$	$A = 0$
$H_1 :$	$A < 0$	$A < 0$

First, we perform a parametric statistical hypothesis test, the **Z-test**, to determine whether the **mean** across the galaxy sample of the estimated slopes, $\bar{A} = \sum_i A_i / N$, is or not significantly lower than $\bar{A} = 0$. This parametric test assumes a normal distribution for the slopes A_i . The test statistic $Z = \bar{A} / \sigma'(A)$ is calculated from the mean and its standard uncertainty $\sigma'(A) = \sigma(A) / \sqrt{N}$, the ratio of the standard deviation $\sigma(A)$ to the square-rooted sample size N . To determine the level of significance we compare the probability (p -value) of observing the mean \bar{A} under the hypothesis H_0 , that there is no tapering, to a level of significance α , and reject the null hypothesis when $p < \alpha$ which would establish the Keplerian behaviour.

Because it is *a priori* not known whether the galaxy-end slopes $A = v'(r)$ are normally distributed, we need a second diagnostic. The null hypothesis of such second test will be to assume the **median** of all slopes to be zero, that is, it

asserts that each individual-galaxy slope has either sign with equal 50 % probability (independently of its absolute value). The alternative hypothesis H_1 , on the contrary, states that the $v(r)$ curves fit to data decrease, that is, in the alternative hypothesis the majority of data will fall on the negative side where $A = v'(r) < 0$, as within an NFW halo.

To contrast these two hypotheses we have chosen a natural non-parametric test, the so-called **sign test**. It evaluates the symmetry of the distribution around $A = 0$.

We calculate the number of values N_+ in our slope set $[A_1, A_2, \dots, A_k]$ that are positive, and also the number of those below 0, denoted in turn as N_- . Our fitted-slope data set will approximately follow a binomial distribution, where each data point has a probability q to be below zero; the total number of galaxies with negative terminal slope then follows a binomial distribution $N_- \propto \text{Binomial}(N, q)$.

If the null hypothesis is true, we are to accept a probability of $q = 50\%$ for any one galaxy to have either increasing or decreasing end velocity, and we expect that approximately half of the slopes are negative (as we have set the median value to be tested at $A = v'(r) = 0$, Rubin's flat rotational curves). If the probability is statistically different from $1/2$, the data will reject the null hypothesis and possibly favour the NFW behaviour.

We test for significance by computing the p -value for the binomial distribution. When the p -value is lower than a certain critical value previously chosen by the investigator we say that there is enough evidence to conclude that the median is below 0, we reject the null hypothesis H_0 and conclude with enough evidence to accept the alternative hypothesis H_1 .

We choose this critical value for p as 0.05 (95 % confidence).

However, if the opposite were true, and the p -value larger than 0.05, we would say that we could not reject the null hypothesis of flat rotation because of scant evidence to confirm that the median of the slopes is lower than 0. Strictly speaking, this would not prove H_0 to be true either, there would just not enough evidence to discard it.

The result of these two tests will be given presently in Section 3.

But before, we propose a second non-parametric test to contrast both hypotheses: the **Wilcoxon test**. This test is designed to look for evidence on whether the median of the distribution of the galactic-slopes set is significantly different from zero, irrespective of whether larger (increasing $v(r)$) or smaller (decreasing $v(r)$) than 0. The test does not assume a normal Gaussian distribution from which the data is sampled, but a symmetric distribution with equal tails to the sides of its median (which the sign test does not, of course). The null hypothesis is here that the data for A is symmetric around 0 (Rubin value). The one-sided alternative hypothesis is then taken as the data being symmetric respect to some median value which is negative (NFW-type of value).

3. Results

3.1. Sensitivity to the value of A_{\max} from Eq. (7)

In the first order of business, let us discuss the sensitivity to the choice of A of Section 2.1 in Eq. (7). Because the selection of data points to be fit depends on that choice, we need to compare several values of this $A \leq A_{\max}$ condition, used to select galactic data points where the rotation curve starts bending towards either a constant or a negative slope, as opposed to the positive one typically displayed by the inner-most points of a galactic rotation curve.

With this intention we test 10 values of A_{\max} ranging between 0 and 1. Then, we rank the linear models represented by each of those values from best to worst in Table 1. For each galaxy we rank each of the 10 models by their χ^2/dof value, to then compute the average rank (Avr rank) for each model across all galaxies.

The lowest that average rank, the better the performance of the model. In the table we see that most of the models have a very similar average rank, so we expect them to similarly describe the rotation data.

In order to understand the agreement among galaxies on the ranking which they assign to each of the values of A_{\max} , we deploy Kendall's W test. While the average rank informs about the mean position of each model across galaxies, Kendall's W reports the consistency of the order of models across galaxies.

The concordance coefficient $W = 12S/(mn^3 - mn)$ is calculated from $m = 93$ the number of galaxies that the 10 models have in common, $n=10$ the number of models, and $S = \sum_{i=1}^n (R_i - \bar{R})^2$, the sum of the ranks R_i and the mean of the ranks \bar{R} for each model. The coefficient W takes values range between 0 (full disagreement) and 1 (full agreement).

We obtain a very low $W = 0.001$, which means that there is little agreement in the models' rankings between galaxies: different values of A_{\max} do better in describing different subsets of the galaxies, with no clear preference.

Indeed, when many galaxies ranks the values of A_{\max} differently, the average rank can be close to a middle value (5 out of 10 in this case), but the rankings are not consistent across galaxies. All the values of the maximum slope at which we start considering that we enter the final tail of the rotation curve perform very similarly, so beyond choosing a natural one, we examine the p -value trend that arises from all of them, as seen in Table 1.

Ranking	A_{\max}	Avg rank	binomial p -value	Wilcoxon p -value	normal p -value	# of galaxies	$A < 0$
1	0.4	5.34	0.84	0.64	0.53	101	46
2	0.6	5.39	0.88	0.73	0.57	103	46
3	0.0	5.42	0.50	0.45	0.48	93	47
4	0.2	5.43	0.66	0.57	0.55	99	48
5	0.1	5.46	0.62	0.54	0.53	96	47
6	0.3	5.46	0.79	0.63	0.52	101	47
7	0.7	5.55	0.86	0.78	0.65	106	48
8	0.8	5.61	0.96	0.93	0.78	113	48
9	0.9	5.64	0.98	0.96	0.83	115	47
10	1.0	5.66	0.98	0.98	0.88	116	47

Table 1: Set of models characterized by A_{\max} (in km/(s kpc)) ordered from best to worse; their average rank (according to the 93 galaxies that the models have in common); their p -values for different statistical tests (non-parametric sign & Wilcoxon tests, and a parametric Z-test); the number of galaxies which remain in each model and the number of galaxies with a decreasing slope $A < 0$, very close to about half of the total.

The conclusion of the computation in that table is that choosing A_{\max} to be 0.9 is not substantially different from selecting basically any number between 0.5 and 1.0, so it merits no further discussion and we proceed to assess the distribution of slopes.

3.2. Rotation-velocity radial dependence at large distances

After having decided which ones are the far-out data points in each rotation curve as per Section 2.1, the sample size is smaller: about 4/7 of the original 175 rotation curves from the SPARC database pass the cut, in the numbers described in Table 1, leaving out those which have sizeable positive slope basically to the end of the measured rotation curve. Taking those galaxies out somewhat biases the analysis in favour of NFW (negative slope) instead of Rubin's behaviour (flat rotation curve). This happens because the number of galaxies with $A > 0$ is decreased, which is why it appears that selecting the somewhat higher $A_{\max} = 0.9$ is a better compromise than choosing a smaller value thereof. This is because those values of A_{\max} in Table 1 which are closer to zero will typically produce data sets where the general trend of the rotation curve will be to either decrease or stay constant, with a smaller chance to be slightly increasing, but due to a selection bias, so we keep the looser cut.

In Appendix A) a few sample galaxies which do pass that cut are shown; those in figure A.4 have slightly positive velocity slope, those in A.5 rather negative, but many of them compatible with zero within one standard deviation anyway. Plots of the rotation curves of *all* galaxies in the SPARC database and the fitted slopes when appropriate are left for the supplementary material.

Next, as explained in Section 2.2, a $v'(r)$ end derivative is extracted for each of the remaining galaxies, after fitting to Eq. 8. In Figure 2 we represent the distribution of the data in a box plot that extends from the first to the third quantiles: SPARC rotation curves still demonstrate a small preference for rather positive, increasing slopes, than negative ones, but the median is very close to zero, and the interquartile range is narrow, with a width of about 1 km/(s kpc), when the natural slope size (looking at the empirical rotation curves is a much larger 10 km/(s kpc). This means that

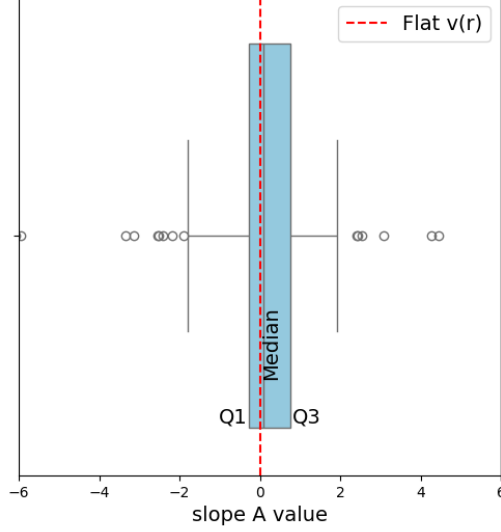


Figure 2: The distribution of terminal slopes $v'(r)$ is symmetrically distributed around $A = 0$, consistently with Rubin’s flat rotation curves. The blue box represents the **interquartile range (IQR)** for the distribution of the slopes fit to the rotation data, from the first (Q1) to the third (Q3) quartiles, and they are comprised within the small range of 1 km/(s kpc) (units of the OX axis). The black line inside that box lies at the median of the $v'(r)$ distribution and is very close to 0. The whiskers extend to $1.5 \times \text{IQR}$ above and below Q1 and Q3, and outside these values we find a few outliers (empty circles).

rotation curves become, statistically speaking, rather flat at the end points.

Then in the left panel of Figure 3 we give the distribution of the fitted SPARC-sample slopes in histogram form, and again see that it is rather peaked around zero. This is corroborated by the smoothed Kernel Density Estimator of the histogram, which is rather well centered at zero. We also plot a Gaussian centered at zero with a deviation of 1 km/(s kpc)

$$N(\mu = 0, \sigma^2 = 1) = \frac{1}{\sqrt{2\pi}} e^{-x^2/2} \quad (10)$$

(units in km, s, kpc) which is seen to be a bit more fat-tailed and less peaked at the center, but close enough to discuss the normal variance of the data. The quality of the Normal-Distribution approximation to the data is given in the corresponding right plot, the quantile-quantile representation, which confirms that the Gaussian approximation is reasonable and one can discuss the distribution in terms of a mean and standard deviation, as well as run a parametric test, the Z-test as described in Subsection 2.3.

This is why we report both parametric (accepting a normal distribution of slopes) and non-parametric (for a sample that does not necessarily follow a normal distribution) hypothesis tests to assess the general trend of the velocity slope sample selected off the SPARC database.

We showed the resulting p -values for the tests on the slope, in addition to the sensitivity to the different choices of A_{max} , in Table 1. That includes the Sign, the Wilcoxon and the Z tests already described. In that same table we find the number of galaxies that display a slightly declining DM rotation curve. The p -value for each A_{max} indicates the position of the sample within the test statistic distribution. A low p -value would suggest that the sample lies in the tail of the distribution, increasing the odds of rejecting the null hypothesis in favour of the alternative (H_1). A higher p -value places the sample near the center of the test statistic distribution, favoring H_0 . In our analysis, all values of A_{max} are conducive to large p values, the smallest of them being 0.45 for the $A_{\text{max}} = 0$ case (in practice demanding

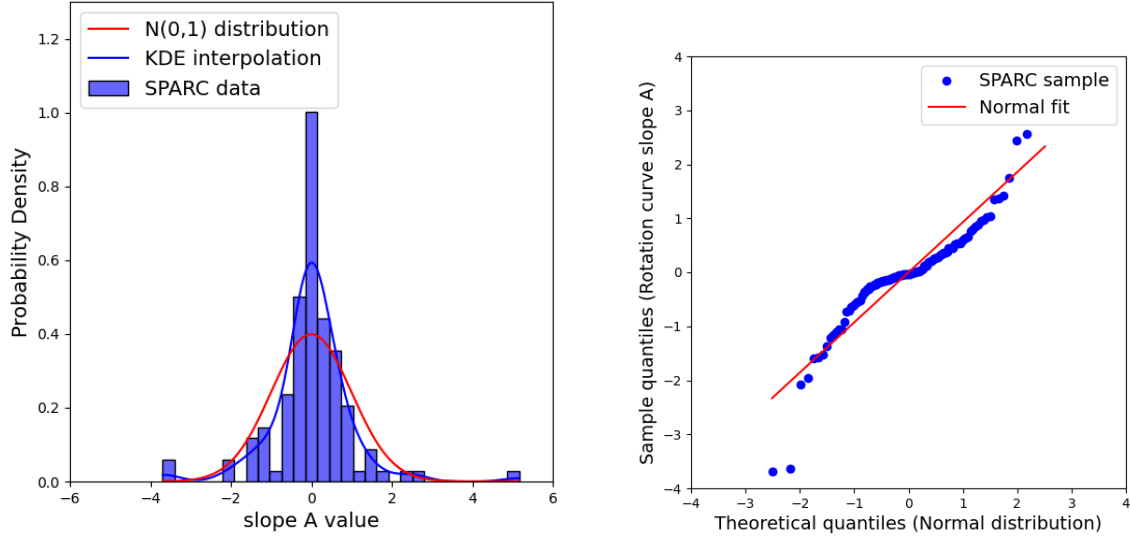


Figure 3: **Left:** Histogram representation of the galactic end slopes together with its smoothing obtained by a Kernel Density Estimation (KDE, blue line) and compared to a normal distribution (red line). The symmetric shape centered near 0, as the statistics tests suggest, is clearly visible by eyeball. **Right:** Quantile-quantile representation to assess whether the slopes are normally distributed as a Gaussian. The data points are sorted and represented against theoretical quantiles from a normal distribution. the red line is the best fit through the points. When the data points are close to the line the data are approximately normal, and this is reasonably the case, lending credibility to the parametric Z test of Subsection 2.3.

for this case that the slope *be negative* in one of the four point segments before even considering the galaxy for the sample!).

The high values of p obtained indicate that the data aligns with the center of their test statistic distributions, rejecting H_1 : the overall behaviour of the database is rather consistent with rotation curves being flat as far as the measurements extend.

To be specific, one can quantify how large these p values are by comparing them to conventional significance thresholds $\alpha = 0.05$ (95% significance) and 0.01 (99% significance). Since the obtained p values are way larger than both 0.05 and 0.01 , we fail to reject the null hypothesis (H_0) with any confidence.

As a result, there is no statistical evidence to conclude that the slope tends to decrease for large r , and the galactic rotation curves lend no support to the NFW-halo picture at large r . In this analysis we very clearly fail to reject H_0 , as SPARC data provides no support for the alternative hypothesis H_1 – decreasing behaviour in the final points of the rotation curve–, over a constant $v(r)$ trend, the H_0 hypothesis.

4. Summary and conclusions

In this analysis we have tested the behaviour of the final points in the rotation curves for the SPARC data set with the intention of discriminating between (i) a decreasing behaviour, typical of Keplerian orbits and expected in Navarro-Frenk-White spherical halo models and (ii) a steady, non-decreasing behaviour as described by V. Rubin.

We have left out from the galaxy sample any of them with an indefinitely increasing behaviour, checking the irrelevance of how to choose this data cut in table 1

For each galaxy that passes the cut we have selected the data points at large r at far-out values where baryonic matter does not dominate or has little effect over the shape of the rotation curve. The objective has been to provide information useful for the behaviour of gravity (e.g. MOND-like theories) or to particle physics properties (as simulations depend

on these, and they can output the halo shape and density profile) in a region dominated by dark matter, where baryonic matter is nearly absent.

The final data points for each rotation curve have been fitted to a simple linear function with χ^2 minimisation, comparing the theoretical predictions with the observed data. With the minimisation of the function we have obtained a sample of slopes, $v'(r) = A$, for the remaining galaxy sample. We have evaluated the general trend of the slope on the sample using parametric as well as non-parametric tests, to reach the conclusion that the null hypothesis is preferred within a 95% of confidence. SPARC galaxies do not show a strong preference in favour of a decreasing trend in their rotation curve, but rather lean towards a constant rotation curve. In previous works (Bariego-Quintana et al. (2023)) SPARC galaxies already demonstrated a preference of elongated shapes that naturally provide a flat rotation curve over spherical haloes with isothermal profiles only for a small r stretch and that slightly decline later.

DM radii are often quoted to reach distances of order 1 Mpc, but this is at very significantly diminished DM density (if they remained isothermal, with $\rho \propto 1/r^2$, the linear divergence in the total mass integral would quickly exceed the fraction of DM in the universe).

Rotation curves in acceptable spherical DM haloes naturally decrease with power-laws near the Keplerian $v \propto r^{-1/2}$ which must manifest at sufficiently large distances from the galactic center, as seen in Figure 1.

In outer galactic regions where baryonic matter becomes negligible, any decline in the dark matter rotation curve should directly manifest in the total rotation curve, providing a critical test for the NFW profile (and also probing modified gravity (Khelashvili et al., 2024)). The fact that most SPARC galaxies do not support this scenario raises an important question about the shape and distribution of dark matter haloes around galaxies, which has significant implications for dark matter searches and the nature of the dark matter components as reflected in their macroscopic, collective behaviour. Gravitational-lensing measurements far away from the galactic disks, as recently reported (Mistele et al., 2024), might be required to understand the distribution of dark matter around galaxies where the would-be rotation curve seems to stay flat until distances where the concept of galaxy itself is questionable.

Given that our p -values exceed the significance level ($p > \alpha$), we conclude that the null hypothesis (flat rotation) adequately describes the database at 95% confidence level (corresponding to approximately two standard deviations). Even if a stricter significance threshold were applied, the results would remain unchanged.

In summary, we cannot reject a final constant trend, H_0 , because there is not enough evidence to support a decrease in the slope ($A < 0$) of $v(r)$. At the same time, we cannot confirm H_1 (Keplerian taper of $v(r)$), as the statistical analysis does not provide sufficient grounds to conclude that the slope decreases. Thus, while we do not definitely confirm either hypothesis, we establish that our data selection does not provide evidence in favor of H_1 , and the decreasing behaviour in the final points of the rotation curve needed for the NFW to be a credible model of galactic DM haloes remains to be found.

Acknowledgments

The authors thank clarifying exchanges with Jose Beltrán at the Univ. of Salamanca, Tobias Mistele from the Frankfurt FIAS, Alexander Knebe from Univ. Autonoma de Madrid and Alfonso Lazo Pedrajas from Univ. of Valencia. Work partially supported by grant PID2022-137003NB-I00 of the Spanish MCIN/AEI /10.13039/501100011033/

Preprint issued as IPARCOS-UCM-25-039

References

- Adriana Bariego-Quintana and Felipe J. Llanes-Estrada. A precis of dark matter for mathematicians. *Trans. A. Razmadze Math. Inst.*, 178(2): 197–211, 2024a.
- Adriana Bariego-Quintana and Felipe J. Llanes-Estrada. The torsion of stellar streams and the overall shape of galactic gravity’s source. *Astronomy & Astrophysics*, 687:A46, June 2024b. ISSN 1432-0746. doi: 10.1051/0004-6361/202347502. URL <http://dx.doi.org/10.1051/0004-6361/202347502>.
- Adriana Bariego-Quintana, Felipe J. Llanes-Estrada, and Oliver Manzanilla Carretero. Galaxy rotation favors prolate dark matter haloes. DOI: 10.1103/physrevd.107.083524. *Physical Review D*, 107(8), Apr 2023.
- Gianfranco Bertone and Dan Hooper. History of dark matter. *Reviews of Modern Physics*, 90(4), Oct 2018. doi: 10.1103/revmodphys.90.045002. URL <https://doi.org/10.1103/revmodphys.90.045002>.
- Arianna Di Cintio, Chris B. Brook, Andrea V. Macciò, Greg S. Stinson, Alexander Knebe, Aaron A. Dutton, and James Wadsley. The dependence of dark matter profiles on the stellar-to-halo mass ratio: a prediction for cusps versus cores. *Mon. Not. Roy. Astron. Soc.*, 437(1):415–423, 2014. doi: 10.1093/mnras/stt1891.
- Scott Dodelson and Michele Liguori. Can Cosmic Structure Form without Dark Matter? *Physical Review Letters*, 97(23):231301, Dec 2006. doi: 10.1103/PhysRevLett.97.231301.
- G. Efstathiou, A. Lewis, S. Galli, and Planck Collaboration. Planck 2018 Results (VI). Cosmological parameters. *Astronomy & Astrophysics*, 641: A6, Sep 2020. doi: 10.1051/0004-6361/201833910. URL <https://doi.org/10.1051/0004-6361/201833910>.
- Carlos S. Frenk, Simon D. M. White, George Efstathiou, and Marc Davis. Cold dark matter, the structure of galactic haloes and the origin of the Hubble sequence. *Nature*, 317(6038):595–597, Oct 1985. doi: 10.1038/317595a0.
- M. Khelashvili, A. Rudakovskiy, and S. Hossenfelder. SPARC galaxies prefer Dark Matter over MOND. 1 2024.
- Federico Lelli, Stacy S. McGaugh, and James M. Schombert. SPARC: Mass Models for 175 Disk Galaxies with Spitzer Photometry and Accurate Rotation Curves. *Astronomy Journal*, 152(6):157, December 2016. doi: 10.3847/0004-6256/152/6/157.
- Felipe J. Llanes-Estrada. Elongated gravity sources as an analytical limit for flat galaxy rotation curves. DOI: 10.3390/universe7090346. *Universe*, 7(9):346, Sep 2021.
- Mordehai Milgrom. A modification of the Newtonian dynamics as a possible alternative to the hidden mass hypothesis. *The Astrophysical Journal*, 270:365–370, Jul 1983. doi: 10.1086/161130.
- Tobias Mistele, Stacy McGaugh, Federico Lelli, James Schombert, and Pengfei Li. Indefinitely Flat Circular Velocities and the Baryonic Tully–Fisher Relation from Weak Lensing. *Astrophysical Letter Journal*, 969(1):L3, July 2024. doi: 10.3847/2041-8213/ad54b0.
- Julio F. Navarro, Carlos S. Frenk, and Simon D. M. White. A Universal Density Profile from Hierarchical Clustering. *Astrophysical Journal*, 490(2):493–508, December 1997. doi: 10.1086/304888.
- Fabrizio Nesti and Paolo Salucci. The dark matter halo of the milky way, ad 2013. *Journal of Cosmology and Astroparticle Physics*, 2013(07):016, jul 2013. doi: 10.1088/1475-7516/2013/07/016. URL <https://dx.doi.org/10.1088/1475-7516/2013/07/016>.
- Stefano Profumo. *An Introduction to Particle Dark Matter*. Springer, London, 2017. ISBN 2059-7711.
- Vera C. Rubin, W. Kent Ford, and Norbert Thonnard. Extended rotation curves of high-luminosity spiral galaxies. IV. Systematic dynamical properties, Sa to Sc. *The Astrophysical Journal Letters*, 225:L107–L111, Nov 1978. doi: 10.1086/182804.
- Madison Walder, Denis Erkal, Michelle Collins, and David Martinez-Delgado. Probing the dark matter haloes of external galaxies with stellar streams. 2 2024.

Appendix A. Plots of a few rotation curves

In Figures 2 and 3 we show some examples of the fitted rotation curves.

The best-fit linear behavior to the (DM contribution to) the $v(r)$ large- r tail, the main object of study of this article, is shown as a dotted black line. The best fit total rotation curve is the solid line (yellow online) with shaded error regions. The points which pass the tail criterion of Eq. (7) and are thus the fittable data are those immersed in the shaded area (and are displayed red online), with the ones at lower r not considered part of the tail.

Finally, two more lines, dashed-dotted, are added. The usually lowest one (blue online) shows the baryon contribution to the rotation curve calculated with Eq. 3, and the upper one (red online) the derived DM rotation curve, from Eq. 4. Both are given for the entire r range and not only for the tail, for ease of comparison with the overall data.

As can be seen, most are compatible with zero terminal slope (given the uncertainty on $A = v'(r)$). Also, we see that generally speaking, the sensitivity to the choice of Eq. (7) is not a major worry but rather a correction.

The rest of the plots to complete the set of all fit galaxies can be found in the supplementary material.

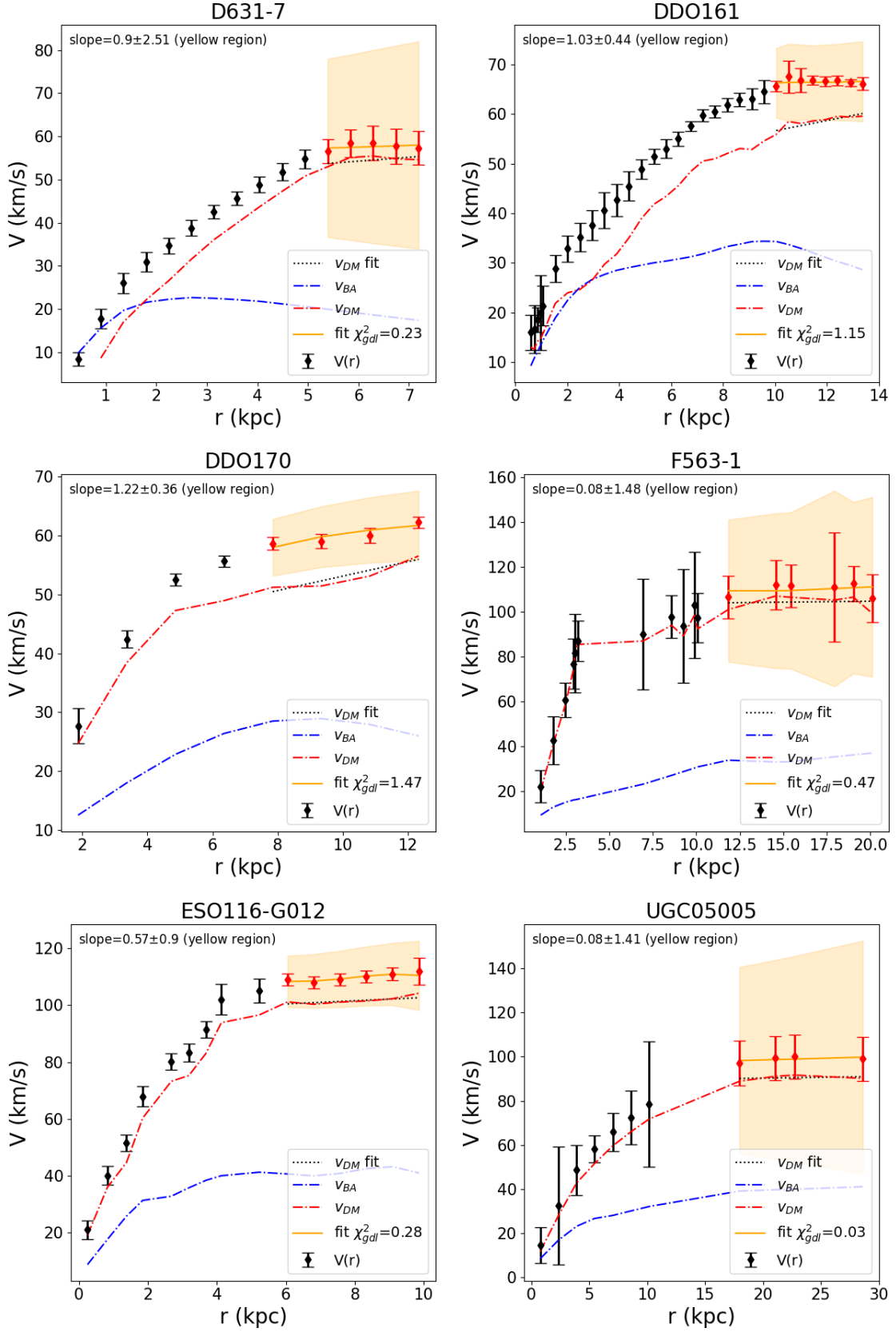


Figure A.4: SPARC rotation curves with slightly positive $v'(r)_{DM}$ slope at large r .

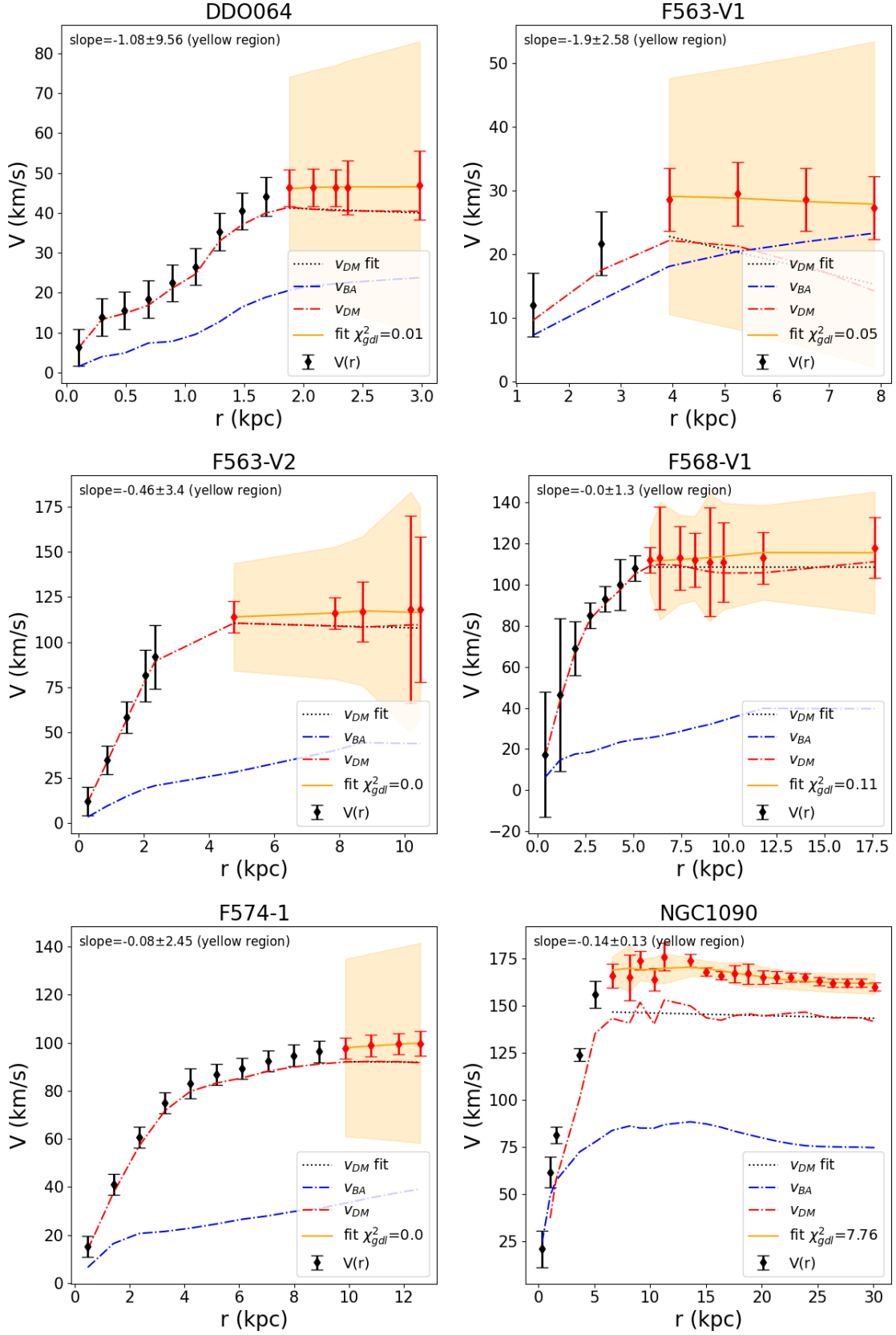


Figure A.5: SPARC rotation curves with slightly negative $v'(r)_{DM}$ slope at large r .